

Extinction of refugia of hantavirus infection in a spatially heterogeneous environment

Niraj Kumar,¹ R. R. Parmenter,² and V. M. Kenkre¹

¹*Consortium of the Americas for Interdisciplinary Science and Department of Physics and Astronomy, University of New Mexico, Albuquerque, New Mexico 87131, USA*

²*Valles Caldera Trust, Jemez Springs, New Mexico 87025, USA*

(Received 19 March 2010; published 22 July 2010)

We predict an abrupt observable transition, on the basis of numerical studies, of hantavirus infection in terrain characterized by spatially dependent environmental resources. The underlying framework of the analysis is that of Fisher equations with an internal degree of freedom, the state of infection. The unexpected prediction is of the sudden disappearance of refugia of infection in spite of the existence of supercritical (favorable) food resources, brought about by reduction of their spatial extent. Numerical results are presented and a theoretical explanation is provided on analytic grounds on the basis of the competition of diffusion of rodents carrying the hantavirus and nonlinearity present in the resource interactions.

DOI: [10.1103/PhysRevE.82.011920](https://doi.org/10.1103/PhysRevE.82.011920)

PACS number(s): 87.23.Cc, 82.40.Ck, 87.15.Zg

I. INTRODUCTION

Abrupt transitions or bifurcations appear in all kinds of complex systems in a variety of sciences ranging from biology and ecology to physics and chemistry. The application of computational methods developed in the latter simpler disciplines to the much more complicated systems encountered in biology and ecology has great value because of the insight into basic mechanisms that the methods can provide. We present such an application in the present paper.

We predict an abrupt transition, observable in principle, in an ecological system related to a topic of substantial current interest, viz., the spatial transmission of epidemics. The source of the transition lies in a blend of nonlinearity, spatial extent, and interaction, and its specific context is the transmission of the hantavirus epidemic. Known technically as the hantavirus pulmonary syndrome (HPS), this rodent-borne zoonotic disease exhibits periodic outbreaks in local or regional settings as a function of complex interactions among host reservoir populations, habitat quality, and climate conditions [1–6]. Human infection risk increases in domestic and peridomestic settings when deer mouse populations increase [4], leading to a time-lagged density-dependent amplification of virus-infected rodents [1]. These events are associated with climate-related drivers (e.g., El Niño-Southern Oscillation dynamics) that increase regional winter-spring precipitation, leading to enhanced rodent food resources and habitat quality [1,5,6], allowing rodent densities and hantavirus infections to rapidly increase and disperse across the landscape.

In the rest of this section, we describe the essential background of hantavirus dynamics, and follow it with a brief introduction of a mathematical model [7–11] that has met with a great deal of success in their theoretical description. In subsequent Sections we use the model along with numerical techniques to predict an abrupt transition, the extinction of infection refugia, and develop a theory to understand the essence of the transition. The purpose of the further development of that theory to be undertaken in subsequent publications will be to provide the mathematical basis for understanding constraints and behaviors of rodent-hantavirus

interactions through time in spatially variable refugia, with the ultimate goal of applying these results to new models of landscape-level disease risk to human society.

Although widely distributed across North America, the deer mouse in the Southwest exhibits habitat preferences for mid- to high-elevation forests, shrublands and grasslands. These habitats are typically found in isolated mountain ranges, and vary in size and distance from one another. The temporal dynamics in habitat quality, resulting from precipitation events, has been quantified using remote-sensing satellite imagery to identify high-risk areas for rodents and hantavirus [12,13,15]. Deer mouse populations and distributions, along with hantavirus infection frequencies, have been hypothesized [7–10] to expand and contract with precipitation regimes in the vicinity of these isolated areas, one of the theoretically predicted consequences being traveling waves of infection [16]. Importantly, these regions have smaller, high-quality core habitat areas, which we term *refugia* because they consistently maintain both high densities of deer mice and hantavirus infections over many years despite extreme climatic fluctuations [13]. Recent monitoring of satellite imagery for evidence of habitat changes in the vicinity of deer mouse refugia has led to successful regional predictions of increased HPS risk to human populations [14]. The analysis below will focus on these infection refugia, in particular their *sudden disappearance* as system parameters are varied across critical values.

The theory developed by some of the present authors for describing the spread of the hantavirus [7–10] has been based on the Fisher equation [17] with internal states representing infection, or its absence, in the mice population. The total mice population is divided into two groups, susceptible labeled by S and infected labeled by I . The evolution equations are [7,8]

$$\begin{aligned}\frac{\partial M_S}{\partial t} &= bM - cM_S - \frac{M_S M}{K} - aM_S M_I + D\nabla^2 M_S, \\ \frac{\partial M_I}{\partial t} &= -cM_I - \frac{M_I M}{K} + aM_S M_I + D\nabla^2 M_I,\end{aligned}\quad (1)$$

and, as is well known, add up to the standard Fisher equation

$$\frac{\partial M}{\partial t} = bM - cM - \frac{M^2}{K} + D\nabla^2 M. \quad (2)$$

Here, t is the time, ∇^2 is the Laplacian describing double differentiation in space, M_S and M_I are, respectively, densities of susceptible and infected mice and $M = M_S + M_I$ is the total mice density, a controls transmission of infection on encounter, b and c are rates of birth and death, respectively, and D is the mouse diffusion coefficient. Crucial to the understanding of the transmission of infection, the latter quantity has been determined for two kinds of hantavirus-carrying mice by combining mark-recapture observations in Panama and Sevilleta, New Mexico, respectively [18,19], in terms of a detailed theory of mice movements [20]. The effect of the environment (food and other resources) is embodied in the environment parameter K . The quantity $K(b-c)$ is commonly known as the carrying capacity. Although it is straightforward to carry out the analysis in any number of spatial dimensions, a $2-d$ description being appropriate because rodents move on the terrain, we present a $1-d$ description in the rest of the paper. This entails the replacement of ∇^2 by the single double partial derivative $\partial^2/\partial x^2$ where x denotes the spatial coordinate. We do this *only* for simplicity since it is easily shown that a $2-d$ description provides no qualitative difference for our purposes. Proportionality factors of the order of 2 introduced by a $2-d$ description are of no practical importance given that the measured quantities in ecological observations in this system have a far greater quantitative uncertainty.

Equation (1) possess the characteristic features of the hantavirus [1] that mice are not born infected and that they are unaffected in any other way (for instance, they do not die faster) when infected. The logistic reaction term in the last of the Eq. (1) is made up of a linear growth term $(b-c)M$ and bilinear depletion term $-M^2/K$. The Fisher description of population dynamics is widespread [21]. The hantavirus model implied by Eq. (1) has been used for a variety of investigations including simulation studies [22], the appearance of traveling waves of infection [16], the extraction of random walk parameters of the rodents [9,20], interesting seasonality effects [23] and other extensions [10].

In their original investigation [7], Abramson and Kenkre showed how crucial the value of the environment parameter K is to the infection. They demonstrated in a space-independent situation that the infected mouse density undergoes a transcritical bifurcation, vanishing when K falls below a critical value K_c . This value is given in terms of the birth and death rates of the rodents, b and c , respectively, and of the infection transmission parameter a [see Eqs. (1)]:

$$K_c = \frac{b}{a(b-c)}. \quad (3)$$

Furthermore, this bifurcation behavior leads in space-dependent situations to the formation of the refugia of infection mentioned above, in regions where $K > K_c$. Refugia are basically spatial patches in which infection survives in off periods of the epidemic. The spatial distribution of resources that leads to these refugia is apparent from Fig. 1 where we show on the left a Landsat satellite image of the Jemez



FIG. 1. (Color online) Left: Landsat satellite image of the Jemez Mountains in northern New Mexico during winter, illustrating the isolated nature of forested mountain ranges in the southwestern United States. The Rio Grande valley is to the right of the image, running from north (top) to south (bottom). Right: Habitats transition along an elevation gradient within the Jemez Mountains (Valles Caldera National Preserve). Deer mouse and hantavirus refugia are typically found within stands of Ponderosa pine/oak and mixed conifer forests, but in high productivity years, mouse populations will increase and expand in spatial extent; in low productivity years, mouse populations shrink in size and distribution, potentially leading to an extinction of the hantavirus infection within an isolated deer mouse population.

Mountains in northern New Mexico during winter. It illustrates the isolated nature of forested mountain ranges in the southwestern United States. The Rio Grande valley is to the right of the image, running from north (top) to south (bottom). The refugia are typically found within stands of Ponderosa pine/oak and mixed conifer forests. It is observed in low productivity years that rodent populations shrink in size and distribution, potentially leading to an extinction of the hantavirus infection within an isolated patch.

The result of the theory [7], is that as K changes, as shown in Fig. 2, from a subcritical value K_b lower than K_c outside a region to a supercritical value K_p higher than K_c within it, the density of infected mice becomes nonzero inside the region (refugium) but falls off to zero as one proceeds out of the

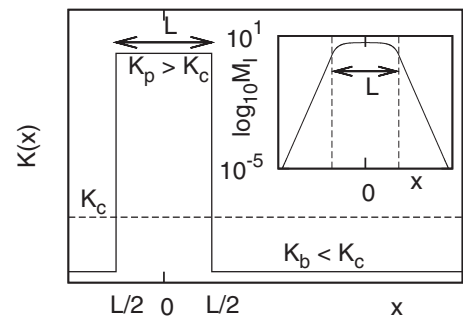


FIG. 2. Step-shaped environmental parameter K with supercritical value $K = K_p$ within the region of width L and subcritical value $K = K_b$ outside the region as shown, the critical value K_c lying between K_p and K_b . The inset shows the steady state infected mouse density M_I obtained numerically by solving Eq. (1) displayed as a log-linear plot: the abscissa in the inset is the distance x (schematic) while the ordinate is the logarithm of M_I . The straight lines away from the supercritical region show that M_I decays essentially in an exponential manner. Parameters used are arbitrary. In appropriate units, $a=0.1$, $b=1.0$, $c=0.5$, $D=20$, $K_p=30$, $K_b=10$, $K_c=20$.

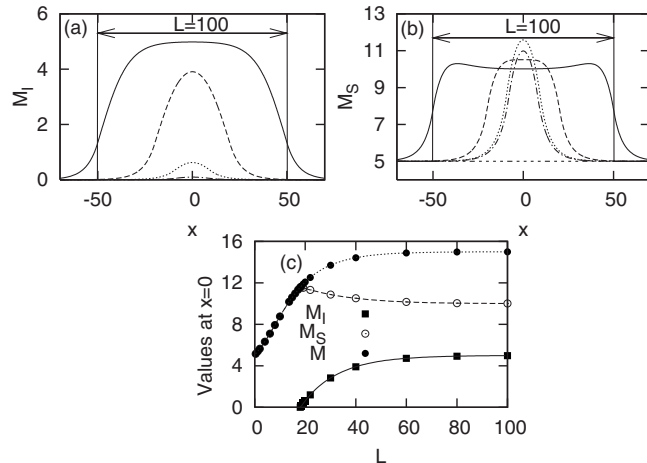


FIG. 3. Abrupt transition in the infection as the extent L of the refugium is varied. Steady state mouse density profiles are shown for different values of L , the infected density M_I in (a) and the susceptible density M_S in (b) respectively. The infected density decreases with a decrease in L ($L=100, 40, 20$ and 18.4 for solid, dashed, dotted and dashed-dotted) and vanishes completely at the critical value, $L=18.2$ in the units employed. The susceptible density, on the other hand, does not vanish even for $L=0$ ($L=100, 40, 20, 16$, and 0 for solid, long-dashed, dotted, dashed-dotted and small-dashed). Values of the densities (infected, susceptible and total) at the center of supercritical region are plotted in (c) as a function of L . Only the infected density exhibits a transition. Parameters are, in arbitrary units: $a=0.1$, $b=1.0$, $c=0.5$, $D=20$.

refugium, the drop-off being gradual as a result of rodent diffusion (nonzero D). This is shown in the inset of Fig. 2, where we use a logarithmic scale for the mice density and see clearly that the drop-off is essentially exponential.

II. NUMERICAL PREDICTION OF EXTINCTION OF INFECTION

Although the drop-off of M_I is gradual from within to outside the region of supercritical K because of diffusion, our numerical studies have recently displayed an abrupt transition in this phenomenon. Let all else be held constant but let the extent of the supercritical region be varied. As this extent falls below a finite critical value, the infection vanishes completely. We display our numerical findings in Fig. 3. The spatial dependence of the infected mouse density M_I is shown in Fig. 3(a) for four different values of the extent L of the supercritical region. It is clear that the lower the value of L , the lower is the amount of infection. What is remarkable is that when L is less than a critical value L_c , which is 18.2 for the given (arbitrary) values of the parameters (see Fig. 2 caption), the infection vanishes *everywhere* including in the supercritical region. This is the transition to which we wish to draw attention.

It appears that the transition we have found from a study of our model might be closely related to what is known as the Island Biogeographic Theory [24] in which it is hypothesized that, when island populations of a particular species become very small, their likelihood of extinction increases

[25]. Concomitant extinction threats increase on smaller islands (that inherently support smaller populations), and on islands more distant from other islands (leading to a lack of recolonization). In the context of deer mouse and *Sin Nombre* hantavirus populations in mountain refugia in the Southwest, similar arguments might lead one to expect that deer mouse populations in smaller, isolated refugia may lose their hantavirus infection when the mouse population becomes too small to maintain infection transmission.

The spatial variation of the noninfected (susceptible) mouse density, M_S , a quantity that *does not* display a transition, is shown in Fig. 3(b). To make the infection transition clear, we plot in Fig. 3(c), the variation of the peak values of M_I , M_S and the total M , in the supercritical region (the refugium) against the extent L . We see the *sharp* disappearance of infection as the peak value of M_I plummets to 0 at a finite value of L . No such behavior occurs for M_S or M . In solving Eq. (1) numerically, we have used an explicit finite difference scheme and have analyzed the convergence to a steady state by measuring the distance between successive solutions. We have taken a periodic boundary condition in a large spatial domain and have taken an initial distribution where the infected and susceptible mouse densities have an initial random value. Other initial conditions give similar results. The (arbitrary) values of other parameters used for the calculations of Fig. 3 are $a=0.1$, $b=1.0$, $c=0.5$, and $D=20$.

The transition means that, if it were desirable to achieve the disappearance of refugia in a given landscape, it would not be necessary to drop the environment resources below the critical value expected in the absence of rodent diffusion. It would suffice to make the spatial extent of the favorable resource regions small enough. The unexpectedness of the result can be appreciated in light of the fact that diffusion is not a one-way process. In principle, it cannot only move infected mice out of the refugium but bring them within it from outside as well.

Extinction transitions related to the spatial variation of parameters in the Fisher equation have been reported earlier [27], including in the study of phytoplankton blooms [26], bacteria in a Petri dish [28–32] and effects of internal fluctuations [33]. While closely related to them (as we shall see below), the transition we report here has the distinguishing feature that it is an *infection* transition rather than one involving the total population of the species. It does not arise from the simple Fisher equation which describes a single density, but from two coupled equations, [Eqs. (1)], one of which describes the evolution of infected mice and the other of susceptible mice. From the steady state spatial density profile for the susceptible mice shown in Fig. 3(b) for five different L values and, it is clear that M_S does not undergo extinction for $L < L_c$. Interestingly, we observe that the profile goes up with increasing L values for $L > L_c$ and, for $L < L_c$ it gradually goes down. Thus, the susceptible density in the middle of the supercritical region shows a peak for $L = L_c$, which reflects the extinction of infected mice density at L_c [see Fig. 3(c)]. For L values very different from the critical length, the M_S values are easily predictable. The respective central values for $L \rightarrow \infty$ and $L=0$, are b/a , equivalently $K_c(b-c)$, as the entire space is then supercritical with $K = K_p > K_c$, and $K_b(b-c)$ as the entire space is then subcritical with $K = K_b < K_c$.

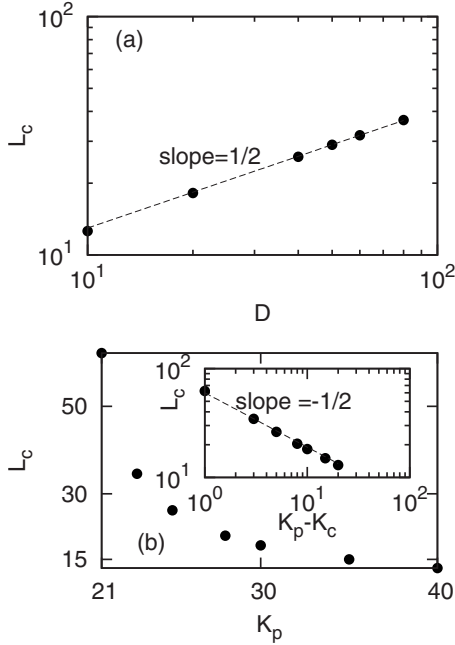


FIG. 4. The critical length L_c plotted for (arbitrary) parameters $a=0.1$, $b=1.0$, $c=0.5$, $K_b=10$ showing power law dependence on (a) the diffusion coefficient D where the plot is on a log-log scale (base 10) and the straight line with slope 1/2 shows the square root power law dependence $L_c \sim \sqrt{D}$, the value of K_p being 30, and on (b) the environmental parameter K_p for the same parameters and $D=20$. Although the main plot in (b) is on a linear scale and shows a complex dependence on K_p , the inset is on a log-log scale (base 10) and against $K_p - K_c$ and the straight line with slope $-1/2$ shows the power law dependence $L_c \sim 1/\sqrt{K_p - K_c}$.

Clearly, it is important to understand the source and nature of the abrupt transition. A common practice in the study of phase transitions is to investigate whether a critical quantity such as L_c depends in a power law fashion on the various parameters of the problem one by one, keeping the other parameters fixed. The nature of the power laws often provides insights about the underlying mechanism for the transition. Careful study of the numerical results indeed reveals an interesting parameter dependence of L_c as shown in Fig. 4. In (a) we see that L_c increases with the diffusion coefficient D as a square root power law: $L_c \sim \sqrt{D}$. In (b) we notice a complex dependence of L_c on the environment parameter K_p which is seen to reduce to an inverse power dependence $L_c \sim (K_p - K_c)^{-1/2}$ near the critical value K_c . These square root dependences provide crucial clues to the underlying mechanism and will guide the theoretical analysis. We have also studied the dependence of L_c on other parameters, specifically, a , b , and c . We have found apparent power law dependence in restricted regimes so that $L_c \sim a^{-2}$, $b^{-2.54}$, and the dependence of L_c on c appears exponential, but these observations are less useful in developing the theory we construct below.

III. THEORETICAL ANALYSIS

As in previous analysis by one of the present authors [8] [see Eq. (51) of that reference], we recast Eq. (1) into equa-

tions for the infected and total mouse densities, eliminating the susceptible density $M_S = M - M_I$. In the steady state, putting the time derivatives equal to zero we obtain, as the starting point of our analysis,

$$D \frac{d^2 M(x)}{dx^2} + (b - c)M(x) = \frac{M^2(x)}{K(x)},$$

$$D \frac{d^2 M_I(x)}{dx^2} + \mathcal{A}(x)M_I(x) = aM_I^2(x). \quad (4)$$

The two differential equations are similar in form but differ in two respects. The total density can be solved without knowledge of the infected density but is required as input into the solution of the infected density, and the linear term for the infected density, given by

$$\mathcal{A}(x) = \left\{ -c + \left[a - \frac{1}{K(x)} \right] M(x) \right\}, \quad (5)$$

is space-dependent whereas in the total density equation, it is the nonlinear term that is inhomogeneous. Our theory in the present paper is based on finding the approximate solution of the total density in Eq. (4), using that solution to obtain a simplified step profile for $\mathcal{A}(x)$ in terms of three parameters as will be explained below, and employing the step profile in an exact analytic argument to deduce extinction conditions for the infected density. We do this in turn below.

A. Finding $M(x)$ through a linearization procedure

If the diffusion coefficient D were to vanish in Eq. (4), the steady state solution for the total density would be $M(x) = K(x)(b - c)$; the other solution, $M(x) = 0$, is an unstable zero. Representing the environment parameter $K(x)$ as a step function as discussed in the context of Fig. 1, with constant values K_p and K_b respectively inside and outside the refugium, we would obtain the result that $M(x)$ is also a step function, with corresponding values $K_p(b - c)$ and $K_b(b - c)$. To determine the total density for finite diffusion coefficient, we expand the solution for $M(x)$ around these values, denoted collectively by M_0 ,

$$M(x) \approx M_0 + \mu(x) \quad (6)$$

and calculate the correction $\mu(x)$ via a linearization procedure which neglects its powers higher than linear. The nature of the linearized equation leads to exponential solutions. Boundary conditions demand that outside the refugium $\mu(x)$ be proportional to $e^{-\alpha|x|}$ to avoid blow-ups at infinitely large distances. Matching logarithmic derivatives at the borders of the refugium, we obtain the required solution for the total mouse density in the linearized approximation:

$$M(x) = K_b(b - c) + \Delta \sinh\left(\frac{\alpha L}{2}\right) e^{-\alpha|x|} \text{ for } |x| > L/2,$$

$$M(x) = K_p(b - c) - \Delta e^{-\alpha L/2} \cosh \alpha x \text{ for } |x| < L/2. \quad (7)$$

The first solution holds outside the extent L of the refugium while the second applies inside the refugium, the difference

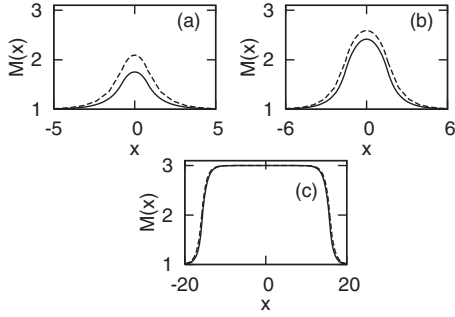


FIG. 5. Validity of the linearization procedure used to obtain the steady state spatial density profile of the total mouse density $M(x)$. Displayed is $M(x)$ expressed in units of $K_b(b-c)$, x being plotted in units of $1/\alpha = \sqrt{D/(b-c)}$. The solid lines are numerically obtained exact solutions of the full nonlinear equation while the dashed lines are the analytically obtained approximation of the linearized counterpart. The three plots, (a), (b), and (c) correspond to three different values of αL ; in (a) it equals 1.58, in (b) it is twice as large as in (a), and in (c) it is ten times as large as in (b). The value of K_p/K_b is 3 in all plots. The procedure clearly becomes more accurate as αL increases.

$(K_p - K_b)(b - c)$ in the carrying capacities inside and outside is denoted by Δ , and $\alpha = \sqrt{(b - c)/D}$ is the reciprocal of the diffusion length of the mice, i.e., is the distance traversed by the random walking mice in the effective growth time $1/(b - c)$.

To study how good this approximation for $M(x)$ is, as we vary αL , the ratio of the refugium length to the diffusion length, we display in Fig. 5 a comparison with exact, i.e., numerically obtained $M(x)$. We find excellent agreement for small diffusion coefficient (large αL) but departures for larger diffusion (small αL). This is expected since it is diffusion that makes $M(x)$ depart from the step function shape of $K(x)$.

B. Representing $\mathcal{A}(x)$ as a step function

The onset of extinction of infection can now be calculated by substituting $M(x)$ as obtained in Eq. (7) in the expression for $\mathcal{A}(x)$ appearing in Eq. (5) followed by the analysis of the second Eq. (4) for M_I . Near the extinction point, one may argue, following an idea proposed by [34] in their budworm work, that the quadratic term in M_I can be safely neglected in favor of the linear term since $M_I(x)$ vanishes at the transition point. This is an exact argument [in contrast to the approximate analysis of the calculation of $M(x)$] that has been recently applied [32] in an unrelated context of the dynamics of bacterial populations. To use that argument in the present infection extinction context, we focus on the second Eq. (4). Extinction requires that $\mathcal{A}(x)$ be negative outside the refugium leading to a depletion rather than growth of infection. The onset of extinction further requires that the depletion rate be large enough in magnitude for the vanishing of infection outside to overwhelm the growth inside the refugium. Among the several possibilities that exist for the construction of an analytic theory, including an approximate Airy function treatment [35] of the problem by representing the x variation

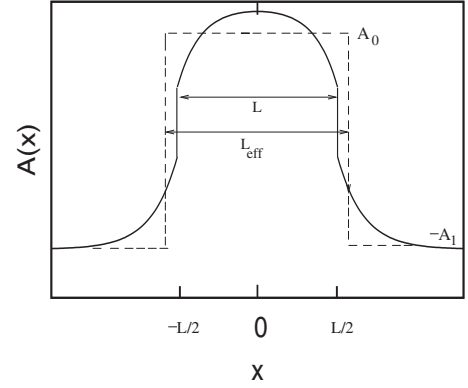


FIG. 6. Schematic representation of the proposed approximation approach for finding the critical length. Plotted is the spatial dependence of $\mathcal{A}(x)$ as obtained from the calculated $M(x)$ (solid line), and in its step profile representation with the constant values \mathcal{A}_0 inside and $-\mathcal{A}_1$ outside the refugium (dashed line). The result is the determination of L_{eff} from the actual L .

of the infection growth term in Eq. (5) as a linear drop, we select here the simplest: we represent $\mathcal{A}(x)$ by a step function with constant values inside and outside the refugium determined by averaging Eq. (5) separately inside and outside the refugium, using the expressions for $M(x)$ we have obtained above.

Figure 6 shows the spatial dependence of $\mathcal{A}(x)$ arising both from the substitution in Eq. (5) of the exponentials in Eq. (7) and the step nature of $K(x)$: the dependence is that of a hyperbolic cosine within the refugium, drops abruptly at the refugium boundaries, and then decays exponentially outside the refugium. Our interest is in replacing this dependence by a simplified step function characterized by three quantities, the two respective values \mathcal{A}_0 and $-\mathcal{A}_1$ of $\mathcal{A}(x)$ inside and outside the refugium, and the effective extent L_{eff} of the refugium. Because $M(x)$ decreases to the value $K_b(b - c)$ and maintains that value throughout the (infinite) extent of the region outside the refugium, it is clear that

$$\mathcal{A}_1 = a(K_c - K_b)(b - c). \quad (8)$$

We obtain the value inside the refugium by averaging $M(x)$ from our expressions Eq. (7),

$$\frac{1}{L} \int_{-L/2}^{L/2} M(x) dx = K_p(b - c) - S(K_p - K_b)(b - c), \quad (9)$$

where S is a switching factor depending only on the ratio of the refugium extent to the diffusion length,

$$S = e^{-\alpha L/2} \left[\frac{\sinh(\alpha L/2)}{\alpha L/2} \right]. \quad (10)$$

The switching factor S varies from 0 to 1 as diffusion increases, the limits being respectively valid for $\alpha L \gg 1$ to $\alpha L \ll 1$. Correspondingly, the average value of $M(x)$ within the refugium varies from $K_p(b - c)$ to $K_b(b - c)$. The general expression for the effective growth rate of infection within the refugium for arbitrary αL is

$$\mathcal{A}_0 = a[(K_p - K_c)(b - c) - S\Delta]. \quad (11)$$

Finally, the effective extent L_{eff} is calculated by equating the area under the approximated step profile (dashed line in Fig. 6), which is $L_{eff}(\mathcal{A}_0 + \mathcal{A}_1)$ to the area under the calculated profile (solid line in Fig. 6) with the consequence that

$$L_{eff} = L \left[\frac{1 - \left(\frac{1}{aK_b} - \frac{1}{aK_p} \right) S}{1 - \left(1 - \frac{1}{aK_p} \right) S} \right], \quad (12)$$

depends on αL as well as on aK_p and aK_b . Although this parameter dependence is quite complex, it is easy to see that L_{eff} is identical to L in the limit of small diffusion coefficient, more appropriately in the limit $\sqrt{D(b-c)}/L \rightarrow 0$ when the switching factor S vanishes. In the same limit, the bracketed factor in Eq. (11) describing \mathcal{A}_0 becomes equal to the carrying capacity within the refugium, $K_p(b-c)$.

C. Determining the onset of extinction of infection

Extinction conditions are now obtained in a straightforward fashion from the representative M_I equations

$$D \frac{d^2 M_I}{dx^2} + \mathcal{A}_0 M_I = a M_I^2, \quad (13)$$

$$D \frac{d^2 M_I}{dx^2} - \mathcal{A}_1 M_I = a M_I^2, \quad (14)$$

by neglecting the quadratic terms (without approximation) because one is interested only in extinction for which they are indeed negligible, solving the linear equations in terms of trigonometric and exponential functions inside and outside the refugium respectively, and matching them at the *effective* boundaries of the refugium. This matching leads to the result that extinction occurs, i.e., infection disappears everywhere, if the refugium extent falls below an effective length given by

$$L_{eff}(L_c) = 2 \sqrt{\frac{D}{\mathcal{A}_0(L_c)}} \arctan \left(\sqrt{\frac{\mathcal{A}_1}{\mathcal{A}_0(L_c)}} \right), \quad (15)$$

where L is replaced by the critical length L_c in the expressions Eqs. (12) and (11) for L_{eff} and \mathcal{A}_0 respectively. Because Eq. (13) is of order 2, both M_I and its derivative are matched, equivalently the logarithmic derivative of M_I . This leads to the arctan factor in Eq. (15). For low diffusion coefficient values, i.e., when $\alpha L \gg 1$, Eq. (15) reduces to the simple explicit formula

$$L_c = 2 \sqrt{\frac{D(b-c)}{a(K_p - K_c)}} \arctan \left(\sqrt{\frac{K_c - K_b}{K_p - K_c}} \right). \quad (16)$$

IV. COMPARISON OF ANALYTIC THEORY TO NUMERICAL SIMULATION

The origin of the power law dependence of the extinction length L_c on the diffusion coefficient D and on the difference $K_p - K_c$ displayed from the numerical simulations in Fig. 4 is now transparently clear from the simple formula, Eq. (16), of our theory. Consider, for instance, the illustrative case in

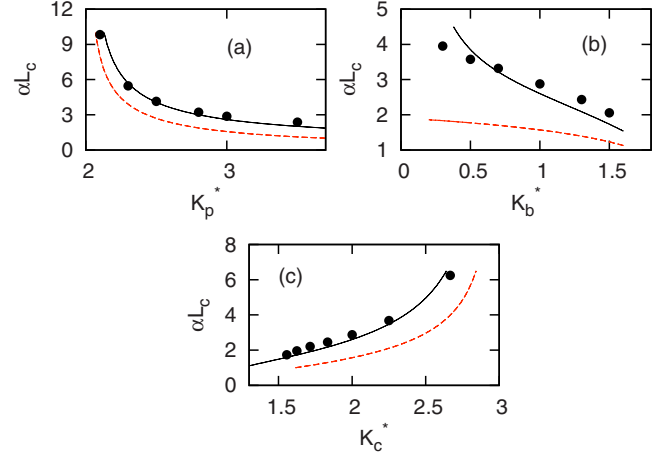


FIG. 7. (Color online) Comparison of our analytic theory with numerically obtained values for the dimensionless extinction length αL_c as a function of the quantities K_p^* , K_b^* and K_c^* in (a), (b), and (c), respectively. In (a), $K_c^* = 2$, $K_b^* = 1$, in (b) $K_p^* = 3$, $K_c^* = 2$ and in (c) $K_p^* = 3$, $K_b^* = 1$. The filled circles are obtained numerically from the full nonlinear time-dependent Eq. (1) and the black solid line is the analytic prediction of our theory as given by Eq. (15). In each of the three figures we also display, as dotted line, the prediction of the simple Eq. (16). That simplified theory qualitatively reproduces the correct behavior and is valid for small diffusion.

which the carrying capacity within the refugium exceeds the critical value by the same amount as the excess of the latter over the carrying capacity outside the refugium. The argument of the arctan is then 1, and the first factor in Eq. (16) clarifies both square root dependences observed in Fig. 4. Although Eq. (16) applies for small diffusion (large αL_c), it captures the essence of the power law. The same tendency is present in the more accurate and general Eq. (15).

Equation (16) that emerges as the small diffusion (large αL_c) limit of the general result Eq. (15), would also be obtained if we had refrained from carrying out the calculation of the steady state total density $M(x)$ [see Eq. (7)] and had simply taken it to be a step function with value $K_p(b-c)$ inside and $K_b(b-c)$ outside the refugium. This would capture some of the essence of the problem but would neglect diffusion. In Fig. 7 we now display the prediction of the simple formula (16) for L_c (dotted line) and find that it describes the qualitative feature of the actual dependence of the extinction length on the environment parameters. The actual dependence, obtained via extensive numerical solutions of the time dependent Eq. (1) in which no linearization is carried out and the parameters varied until extinction is found to occur, is denoted by dark circles in Fig. 7. The abscissa in the three plots is the dimensionless quantity $K_\beta^* = aK_\beta$, with $\beta = p, b, c$. To bring quantitative agreement between theory and simulation, we see that it is important to go beyond the simple expression Eq. (16) and to use the detailed theory resulting in the full formula (15). This is represented by the solid line. We see a satisfactory degree of agreement. The departures arise from the simplifications we have had to make to tackle this very complex extinction problem that can be solved only approximately. By contrast, extinction of total densities, where infection is not involved, that appear for instance in

bacterial population dynamics, are amenable to an exact theory [32].

V. CONCLUSION

The aim of the present paper has been the application of the methods of mathematics and physics to gain insights into an important problem in epidemiology and ecology, following the tradition of interdisciplinary science [36,37]. Our starting point in this paper was Eq. (1) for the dynamics of the rodents responsible for the spread of the hantavirus. Numerical investigations on their basis revealed an extinction transition whose nature is considerably more complex than that of simpler similar phenomena encountered, for instance, in bacterial populations [28–31]. While for those simpler cases one can construct an exact theory [32], it is only possible to develop an approximation scheme to treat the infection transition case. This we have presented here. Our final result is Eq. (15) for the extinction length of the refugium expressed in terms of the rodent diffusion coefficient and carrying capacities. The success of the theory in reproducing features of the transition, including the power law dependence of the extinction length on system parameters, is visually clear from Fig. 7.

A tacit assumption made in the analysis is that the rodents perform ordinary random walks. It is obviously important to ask whether that simplification is valid. Extensive studies carried out by Giuggioli *et al.* [18] regarding the movements of *Zygodontomys brevicauda* in the site in Panama mentioned in that reference and by Abramson *et al.* [19] concerning the movements of *Peromyscus maniculatus* in the site in New Mexico studied in that latter reference have shown that field observations are largely compatible with that assumption within the margin of normal experimental error. We refer the reader particularly to the discussion related to Figs. 4 and 5 of Abramson *et al.* [19]. For any new case, the statistics of the field observations can be examined to ensure that the departure from Gaussian behavior, i.e., the assumption of ordinary random walks, is not too large. If, however, it is found to be significant in a particular case, the effects can be incorporated in principle in the analysis by changing the diffusion equation by introducing an appropriate memory in the transport equation. This is, however, outside the scope of the

present paper. The clear evidence for ordinary random walks found in refs [18,19]. gives us sufficient justification to base our analysis on the diffusion equation alone.

The square root power law behavior originates from the fact that mice perform random walk motion on the terrain. Because the mice are random walkers, their average displacement tends to grow as the square root of the number of steps they take. It is this feature that results in the power law, as is clear from an inspection of the present theory. Quantitative information about the random walks of the mice are available from the published literature. Observational evidence for the quantitative as well qualitative aspects of the random walk movement of the rodents has been gathered in a number of earlier papers. We would like to point out in particular, the study of the movements of the mouse *Peromyscus maniculatus* in New Mexico and clear findings that their diffusion constant is of the order of 475 ± 50 m² per day; and those of the movements of *Zygodontomys brevicauda* in Panama where the mice were found to move slower, viz., with a diffusion constant of 200 ± 50 m² per day. The details of the extraction of the diffusion parameters and the experimental set-ups will be found respectively in Refs. [19,18].

A simple way to interpret our mathematical results in terms of the ecology of the mouse, virus and habitat is to notice that deer mice get infected during fights (horizontal transmission), and that when resources are low, the population of mice declines and reduces the chances of a fight, consequently virus transmission. Thus the total mouse density can remain positive but the infected density can drop to zero. These ideas, basic also to the well-known Island Biogeographic theory [24], find an analytic description in terms of the development presented here. With the theoretical understanding well in hand, it is important to carry out systematic field observations of the extinction transition. We are in the process of collecting such observations, exemplified by plots of the densities of infected mice versus total mice, and hope in the future to present a comparison of the theory to field data.

ACKNOWLEDGMENTS

This work was supported in part by the NSF under Grant No. INT-0336343 and by NIH/NSF under Grant No. EF-0326757.

-
- [1] T. L. Yates, J. N. Mills, C. A. Parmenter, T. G. Ksiazek, R. R. Parmenter, J. R. Vande Castle, C. H. Calisher, S. T. Nichol, K. D. Abbott, J. C. Young, M. L. Morrison, B. J. Beaty, J. L. Dunnum, R. J. Baker, J. Salazar-Bravo, and C. J. Peters, *BioScience* **52**, 989 (2002).
- [2] S. T. Nichol, C. F. Spiropoulou, S. Morzunov, P. E. Rollin, T. G. Ksiazek, H. Feldmann, A. Sanchez, J. Childs, S. Zaki, and C. J. Peters, *Science* **262**, 914 (1993).
- [3] J. E. Childs, T. G. Ksiazek, C. F. Spiropoulou, J. W. Krebs, S. Morzunov, G. O. Maupin, K. L. Gage, P. Rollin, J. Sarisky, R. Ensore, J. Frey, C. J. Peters, and S. T. Nichol, *J. Infect. Dis.* **169**, 1271 (1994).
- [4] J. E. Childs, J. W. Krebs, T. G. Ksiazek, G. O. Maupin, K. L. Gage, P. E. Rollin, P. S. Zeitz, J. Sarisky, R. E. Ensore, J. C. Butler, J. E. Cheek, G. E. Glass, and C. J. Peters, *Am. J. Trop. Med. Hyg.* **52**, 393 (1995).
- [5] R. R. Parmenter, J. W. Brunt, D. I. Moore, and S. Ernest, *The hantavirus Epidemic in the Southwest: Rodent Population Dynamics and the Implications for Transmission of hantavirus-associated Adult Respiratory Distress Syndrome (HARDS) in the Four Corners Region* (Report to the Federal Centers for Disease Control and Prevention, Atlanta, GA, 1993).

- [6] J. N. Mills, *Arch. Virol.* **19**, 45 (2005).
- [7] G. Abramson and V. M. Kenkre, *Phys. Rev. E* **66**, 011912 (2002).
- [8] V. M. Kenkre, in *Modern Challenges in Statistical Mechanics: Patterns, Noise, and the Interplay of Nonlinearity and Complexity*, AIP Conf. Proc. No. 658, edited by V. M. Kenkre and K. Lindenberg (AIP, New York, 2003), pp. 63–102.
- [9] V. M. Kenkre, *Physica A* **356**, 121 (2005).
- [10] V. M. Kenkre, L. Giuggioli, G. Abramson, and G. Camelo-Neto, *Eur. Phys. J. B* **55**, 461 (2007).
- [11] Niraj Kumar, M. N. Kuperman, and V. M. Kenkre, *Phys. Rev. E* **79**, 041902 (2009).
- [12] G. E. Glass, J. E. Cheek, J. A. Patz, T. M. Shields, T. J. Doyle, D. A. Thoroughman, D. K. Hunt, R. E. Ensore, K. L. Gage, C. Ireland, C. J. Peters, and R. Bryan, *Emerg. Infect. Dis.* **6**, 238 (2000).
- [13] G. E. Glass, T. L. Yates, J. B. Fine, T. M. Shields, J. B. Kendall, A. G. Hope, C. A. Parmenter, C. J. Peters, T. G. Ksiazek, C.-S. Li, J. A. Patz, and J. N. Mills, *Proc. Natl. Acad. Sci. U.S.A.* **99**, 16817 (2002).
- [14] G. E. Glass, T. M. Shields, R. R. Parmenter, D. Goade, J. N. Mills, J. Cheek, J. Cook, and T. L. Yates, Museum of Texas Tech University Occasional Paper No. 255, 2006 (unpublished).
- [15] G. E. Glass, T. Shields, B. Cai, T. L. Yates, and R. Parmenter, *Ecol. Appl.* **17**, 129 (2007).
- [16] G. Abramson, V. M. Kenkre, T. L. Yates, and R. R. Parmenter, *Bull. Math. Biol.* **65**, 519 (2003).
- [17] R. A. Fisher, *Ann. Eugen. London* **7**, 355 (1937).
- [18] L. Giuggioli, G. Abramson, V. M. Kenkre, G. Suzane, E. Marce, and T. L. Yates, *Bull. Math. Biol.* **67**, 1135 (2005).
- [19] G. Abramson, L. Giuggioli, V. M. Kenkre, J. W. Dragoo, R. R. Parmenter, C. A. Parmenter, and T. L. Yates, *Ecol. Complexity* **3**, 64 (2006).
- [20] L. Giuggioli, G. Abramson, V. M. Kenkre, R. R. Parmenter, and T. L. Yates, *J. Theor. Biol.* **240**, 126 (2006).
- [21] J. D. Murray, *Mathematical Biology*, 2nd ed. (Springer, New York, 1993).
- [22] M. A. Aguirre, G. Abramson, A. R. Bishop, and V. M. Kenkre, *Phys. Rev. E* **66**, 041908 (2002).
- [23] K. Lindenberg, C. Escudero, J. Buceta, and F. J. de la Rubia, *Proc. SPIE* **5467**, 98 (2004).
- [24] R. H. MacArthur and E. O. Wilson, *The theory of island biogeography* (Princeton University Press, Princeton, NJ, 1967), p. 203.
- [25] J. H. Brown and M. V. Lomolino, *Biogeography* (Sinauer Associates, Inc., Sunderland, MA, 1998).
- [26] M. Kot, *Elements of Mathematical Ecology* (Cambridge University Press, Cambridge, England, 2003).
- [27] J. G. Skellam, *Biometrika* **38**, 196 (1951).
- [28] V. M. Kenkre and M. N. Kuperman, *Phys. Rev. E* **67**, 051921 (2003).
- [29] A. L. Lin, in *Modern Challenges in Statistical Mechanics: Patterns, Growth, and the Interplay of Nonlinearity and Complexity*, AIP Conf. Proc. No. 658 edited by V. M. Kenkre and K. Lindenberg (AIP, New York, 2003).
- [30] A. L. Lin, B. Mann, G. Torres, B. Lincoln, J. Kas, and H. L. Swinney, *Biophys. J.* **87**, 75 (2004).
- [31] N. Perry, *J. R. Soc., Interface* **2**, 379 (2005).
- [32] V. M. Kenkre and Niraj Kumar, *Proc. Natl. Acad. Sci. U.S.A.* **105**, 18752 (2008).
- [33] C. Escudero, J. Buceta, F. J. de la Rubia and K. Lindenberg, *Phys. Rev. E* **69**, 021908 (2004).
- [34] D. Ludwig, D. G. Aronson, and H. F. Weinberger, *J. Math. Biol.* **8**, 217 (1979).
- [35] N. Kumar and V. M. Kenkre, e-print [arXiv:0811.2232v1](https://arxiv.org/abs/0811.2232v1).
- [36] S. A. Levin, *Annu. Rev. Ecol. Syst.* **7**, 287 (1976).
- [37] S. P. Petrovskii and B. L. Li, *Exactly Solvable Models of Biological Invasion* (Chapman and Hall, London/CRC Press, Boca Raton, FL, 2006).